物理參數化對RSM側邊界鬆弛法之敏感度分析

Sensitivity Analysis of Physics Parameterizations to Lateral Boundary Relaxation Method of RSM

陳映如[1,2] (Chen Y.-J.) 莊漢明[2,3] (Juang H.-M. H.) 陳建河[1] (Chen J.-H.)

[1]中央氣象局資訊中心 [2]國立中央大學大氣科學系 [3]美國國家環境預測中心

[1] Meteorological Information Center, Central Weather Bureau

[2] Department of Atmospheric Sciences, National Central University

[3]Environmental Modeling Center, National Centers for Environmental Prediction

摘 要

側邊界條件的設置與數值處理一直是區域模式發展的一大議題，對此，RSM以擾動量濾波模式(perturbation filtering model)的概念設計，將整個模擬範圍區域嵌套(domain nesting)於全球模式中，並取全場(full field)與來自全球模式的背景場(base field)差值為擾動量，因此在長期積分中，RSM可保有大尺度環流不會偏離全球模式的優勢，且能模擬全球模式網格無法解析的中小尺度擾動。

雖然RSM的背景值不是來自側邊界，但是側邊界的數值處理對於模式穩定度仍是重要的，因此RSM使用側邊界鬆弛法來抑制模擬邊界上擾動量的增長。而在測試高解析度RSM 5公里嵌套CWBGFS 25公里的過程中，我們發現在有天氣系統(如颱風)移入RSM模擬範圍時，RSM使用的側邊界鬆弛法係數分布對於物理參數化法反應程度有明顯影響，因此我們將探討，在不同側邊界鬆弛法係數設定中，物理參數化法對於在邊界附近受不同尺度作用的反應程度差異與敏感度測試。

關鍵字：側邊界鬆弛法、物理參數化法之尺度敏感度

Abstract

Numerical methods and proper lateral boundary conditions have always been crucial for the development of regional models. By domain nesting strategy, RSM works as a perturbation filtering model having its perturbation field from the subtraction of base field from the full field. Since the base field is provided by global model during the integration, the large-scale circulation in RSM is preserved as it is in global model, and more small-scale phenomena can be simulated in RSM due to higher resolution setting.

Although the base field of RSM depends on domain nesting instead of lateral boundary, it is important to apply lateral boundary relaxation to constrain the growth of perturbation to avoid instability near the boundary. During some case studies with high resolution (5 km) RSM nested in 25 km CWBGFS, we found that when there are some synoptic systems, like tropical cyclones, entering the domain of RSM, there are some inconsistent responses from physics parameterization due to the effect of lateral boundary relaxation method. Thus, this paper will focus on the sensitivity analysis of the responses of physics parameterizations to the forcing with different scales depending on the relaxation coefficients.

Key words: lateral boundary relaxation method, scale-sensitivity of physics parameterization

1. Introduction

Over the past few years, many numerical experiments have been conducted using RSM (Regional Spectral Model; Juang and Kanamitsu 1994; Juang et al. 1997) nested in CWBGFS (Central Weather Bureau Global Forecast System). Two primary settings adopted were RSM 12km nested into 55 km fully coupled global atmosphere-ocean model for 13-month short-term climate forecasts, and RSM 5km nested into 25 km global atmosphere model with one-dimensional ocean model for 45-day extended weather forecasts.

RSM is a regional model that adopts domain nesting strategy and functions as a perturbation filtering model. The perturbation field of RSM is calculated from the subtraction of base field from the full field. The small-scale perturbation in RSM would start to evolve during the integration because of the higher resolution and finer terrain configuration. On the other hand, the base field is provided by global model during the integration, so the large-scale circulation in RSM is preserved as it is in global model. Although the base field of RSM relies on the whole domain rather than merely the lateral boundary, the lateral boundary continues to play an important role in model stability.

The lateral boundary treatment applied in RSM is implicit lateral boundary relaxation (Juang et al. 1997), which helps constrain the growth of perturbation at the lateral boundary. Nonetheless, we found that the profile of the lateral boundary relaxation coefficient would also influence the weather system entering the simulation domain, especially for high resolution experiments. For example, during some case studies with high resolution (5 km) RSM nested in 25 km CWBGFS, we found that when there was a tropical cyclone entering the domain, there would be some inconsistent responses from physics parameterizations due to the effect of lateral boundary relaxation method. These inconsistent responses would further impact the tropical cyclones' structure in respect of the shape of eyewall and the surrounding rainbands. Also, some grid-point storms or storms smaller than 50 km in radius had a great chance to occur in these simulations. Thus, this paper will discuss the impact of this boundary treatment and the responses of different physics parameterizations, especially the deep convection schemes, to different lateral boundary relaxation profiles.

2. Methods

I. model configuration

Regional Spectral Model (RSM) 5km was used in this study, and the initial data and base field were from CWBGFS $T_{Co}383L72$, which was developed for extending weather forecasting in CWB.

RSM used three-time-level non-iteration dimensional-split Semi-Lagrangian (NDSL; Juang 2007; Juang 2008) scheme and had 42 σ vertical layers. The horizontal domain was shown in FIG. 2. The 4^{th} order horizontal diffusion was utilized and a forward-weighted coefficient 0.7 was applied to the semi-implicit scheme. The integration timestep of this RSM 5km setting was 45 seconds. Two deep convection parameterization schemes, new Tiedtke scheme and scale-awareness SAS scheme, were applied respectively and the differences in their responses to the lateral boundary relaxation method were compared. Except the deep convection schemes, other parameterizations were the same among all the experiments. The radiation scheme included RRTM long-wave radiation and M-D Chou's short-wave radiation scheme. The microphysics scheme was Zhao and Carr (1997). The land surface model in RSM was Noah LSM, and the vertical diffusion scheme used was YSU.

II. lateral boundary relaxation coefficients

Three different profiles of lateral boundary relaxation coefficients (as shown in FIG. 1) were used in this study to test the sensitivity of responses of physics parameterizations. The original profile of the lateral boundary relaxation coefficient depended on the distant ratio to the 15^{th} power (FIG. 1, blue solid line labeled as "pow15"), which had about 15% of the half-domain influenced by the lateral boundary relaxation. Another steeper profile "pow50" (FIG. 1, orange dotted line) had a narrower lateral boundary relaxation zone (about 5% of

the half-domain). The other "smooth_gaussian" (FIG. 1, gray dashed line) profile put a very large region (16% of half-domain) under strong lateral boundary relaxation condition (coefficients were equal to one), and about 33% of the half-domain was influenced by the relaxation scheme. This "smooth_gaussian" profile was designed to set the edge of relaxation zone apart from the boundary of the simulation domain to better examine the transition responses of the cumulus schemes.

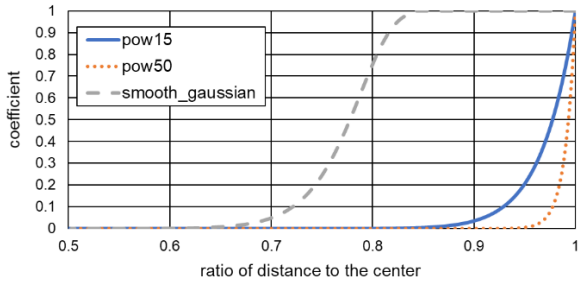

FIG. 1 Three profiles of lateral boundary relaxation weighting coefficients. The horizontal axis shows the ratio of distance to the simulation center, so the larger the ratio, the closer to the lateral boundary.

3. Results and Discussion

The lateral boundary relaxation was applied to all the prognostic variables, which restricted the growth of perturbation adjacent to the boundary. Thus, the relaxation scheme helped stabilize the model and also forced the fields in RSM to resemble their base fields which were from CWBGFS. From the case studies of Typhoon Mangkhut (2018), we found that while the tropical cyclone (TC) was entering the domain, the structure of the simulated TC was twisted, and some grid-point storms formed along the spirals of the cyclone. Moreover, the broader the relaxation zone, the later the cyclone started to enhance. Since the base fields were identical in every experiment, the differences depended on the extent to which the perturbation had evolved. Due to the differences in small-scale forcing, the responses of the physics parameterizations were expected to perform differently. In this paper, we focused on revealing the responses of two different deep convection schemes – new Tiedtke scheme and scale-awareness SAS scheme.

I. sub-grid scale precipitation

The major differences observed between the results of new Tiedtke and scale-awareness SAS were the sub-grid scale precipitation. When new Tiedtke scheme was applied, discontinuous sub-grid scale precipitation crossing the inner domain and the relaxation zone was conspicuous. For example, in FIG. 2 (a) and (b), alone $16^{o}N$, from $138^{o}E$ to $142.477^{o}E$, the sub-grid scale precipitation suddenly increased from below 1 mm to over 6 mm and dropped back to around 4 mm. The edge of abundant sub-grid scale precipitation aligned with the edge between the inner domain and the relaxation zone, where the coefficient of relaxation dropped to zero. Therefore, the narrower the relaxation zone, the thinner the area of rich sub-grid scale precipitation. On the other hand, the simulation using scale-awareness SAS in FIG. 2 (c) and (d), showed an unclear relation between the area of sub-grid scale precipitation and the relaxation zone. Also, unlike new Tiedtke scheme, scale-awareness SAS tended not to precipitate in the relaxation zone close to the south-east border of the simulation area.

II. Structure of tropical cyclone

In both experiments using new Tiedtke and scale-awareness SAS, TCs entering the simulation domain were twisted to a more polygon-like shape and were occasionally accompanied by some grid-point storms (FIG. 2). The polygon-like shape was probably because of the southern simulated boundary that restricted the flow, and also, the changing scales of the forcing across the inner domain and the relaxation zone might also play a role. The latter conjecture seems more plausible in experiments with "smooth_gaussian" profile (FIG. 1 gray dashed line). For instance, FIG. 3, FIG. 4, and FIG. 5 show how the TC structure changed when it went across the edge of the relaxation zone. In FIG. 3, the major portion of TC was located in the relaxation zone. Although the TC was close to the southern simulation boundary, it remained relatively symmetric. The asymmetric shape happened when there was nearly half of the TC circulation locating in the inner domain, whereas about half of the circulation remained in the relaxation zone (FIG. 4). In the experiments using new Tiedtke scheme (FIG. 3 (a), FIG. 4 (a) and FIG. 5 (a)), more sub-grid scale precipitation was produced and more cloud water was generated at the upper atmosphere compared to scale-awareness SAS scheme (FIG. 3 (b), FIG. 4 (b) and FIG. 5 (b)).

It is also hypothesized that since new Tiedtke scheme consumed more instability to precipitate than the scale-awareness SAS did, there were actually less grid-point storms (FIG. 5 (b)) forming in the results of new Tiedtke scheme (FIG. 5 (a)), though the shape of TC also become polygon-like.

4. Conclusion

The different profiles of lateral boundary relaxation and the corresponding responses of new Tiedtke and scale-awareness SAS deep convection schemes were discussed. The cases used in this study were the simulation of Typhoon Mangkhut (2018). From the experiments, we found that (1) new Tiedtke scheme produced more sub-grid scale precipitation than scale-awareness SAS in the relaxation zone, in which the large-scale circulation of the base field dominated the forcing and the small-scale perturbation was limited. (2) New Tiedtke acted very differently across the edge of relaxation zone, but the responses of scale-awareness SAS were similar. (3) The wider and smoother the lateral boundary relaxation were, the slower the tropical cyclone entering the simulation domain intensified. (4) Less grid-point storms were formed in the new Tiedtke experiments than scale-awareness SAS experiments. Several hypotheses were proposed to explain these phenomena:

1. New Tiedtke scheme was more sensitive to the transition of the scales of the forcing across the edge of relaxation zone than scale-awareness SAS scheme.
2. Due to less small-scale perturbation involvement, the tropical cyclone intensified slower in the relaxation zone.
3. New Tiedtke scheme causing more sub-grid scale precipitation might consume more instability than scale-awareness SAS, which decreased the numbers of the grid-point storm formation.

The mechanism and process involving in these phenomena was not fully analyzed in this study. More specific experiments and methods were needed to examine these hypotheses.

References

Juang, H.-M. H., and M. Kanamitsu, 1994: The NMC nested regional spectral model. *Mon. Wea. Rev.*, **122,** 3–26.

Juang, H.-M. H., S.-Y. Hong, and M. Kanamitsu, 1997: The NCEP regional spectral model: An update. *Bull. Amer. Meteor. Soc.*, **78,** 2125– 2143.

Juang, H-M. H., 2007: Semi-Lagrangian advection without iteration. *Proc. Conf. on Weather Analysis and Forecasting*, Longtan, Taoyan, Taiwan, Central Weather Bureau, 277.

Juang, H-M. H., 2008: Mass conserving and positive semi-Lagrangian tracer advection in NCEP GFS. *Proc. Conf. on Weather Analysis and Forecasting*, Taipei, Taiwan, Central Weather Bureau, 225–227.

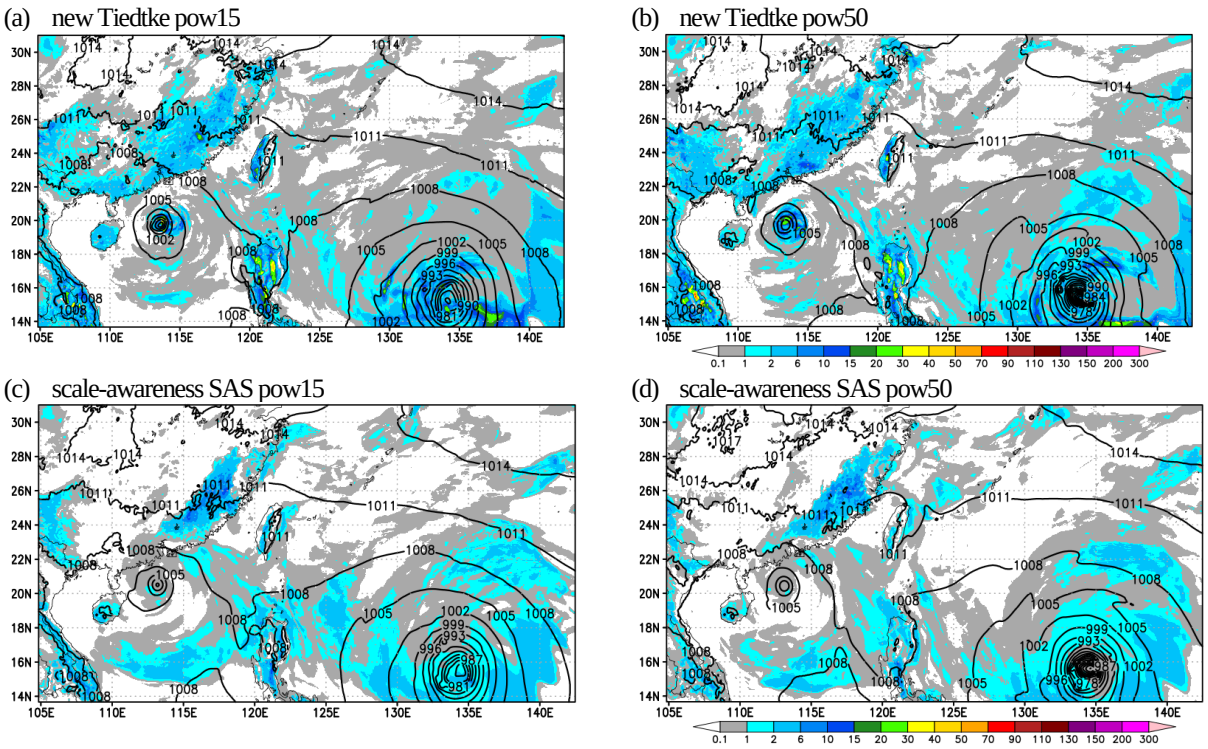

FIG. 2 Sub-grid scale precipitation of new Tiedtke scheme (a, b) and scale-awareness SAS scheme (c, d) with two different relaxation profiles shown in FIG. 1. These are 36 hr forecast of the case with initial time at 00 UTC 2018 Sept. 11.

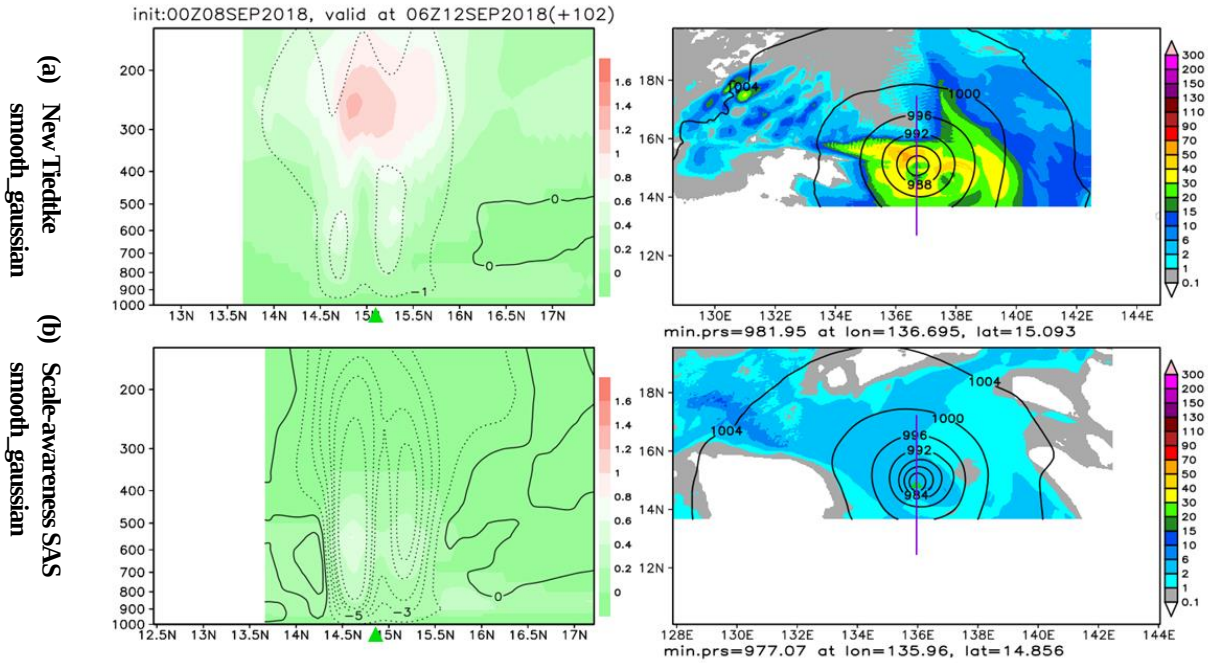

FIG. 3 Simulation results at 102 forecasting hours using "smooth_gaussian" profile illustrated in FIG. 1 gray dashed line. The left panels are vertical profile of the vertical wind speed (Pa/s; contour levels are -15, -10, -8, -5, -3 -1, 0, 1, 3, 5, 8, 10, 15 and the negative values are presented in dashed line.) and cloud water (10^3 kg/kg) of the purple segments in the right panels, and the right panels are horizontal distribution of 6-hour accumulated total precipitation (mm) and mean sea level pressure (hPa). The white margins are areas out of the simulated domain. The green triangle marks the location of minimum mean sea level pressure.

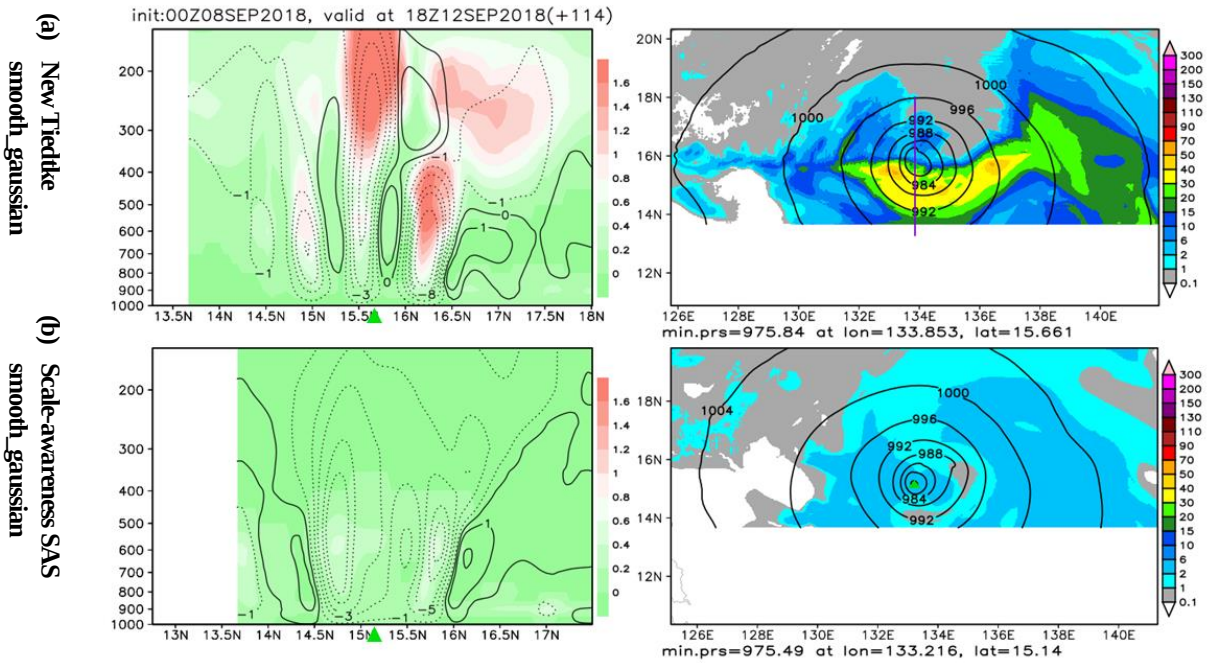

FIG. 4 Same as FIG. 3 but at 114 forecasting hours.

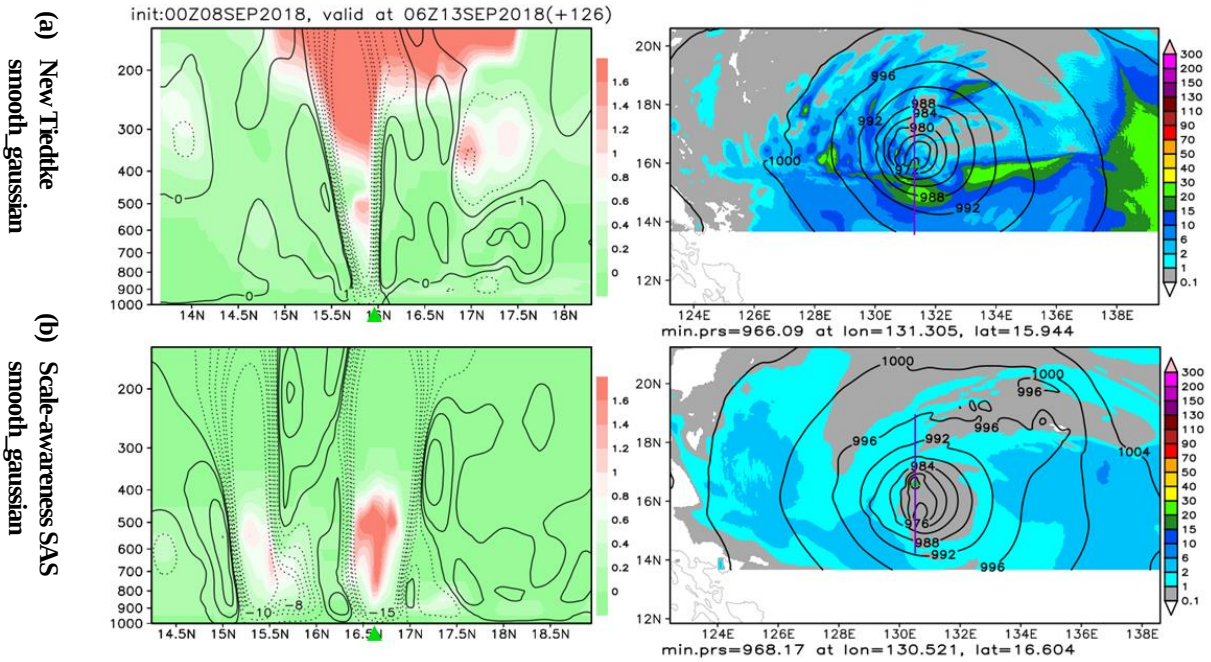

FIG. 5 Same as FIG. 3 but at 126 forecasting hours.